1. High-fidelity finite element models of composite wind turbine blades with shell and solid elements

Authors: Mathijs Peeters[1,*], Gilberto Santo[2], Joris Degroote[2] and Wim Van Paepegem[1]

1 - Department of Materials, Textiles and Chemical Engineering, Ghent University, Tech Lane Ghent Science Park – Campus A, Technologiepark-Zwijnaarde 903, 9052 Zwijnaarde

2- Department of Flow, Heat and Combustion Mechanics, Ghent University, Sint-Pietersnieuwstraat 41 – 9000 Ghent, Belgium

* Correspondence: Mathijs.Peeters@UGent.be

Abstract: A novel approach for creating highly detailed finite element models of wind turbine blades is presented. The approach is implemented as a software tool which handles all the different steps of the model creation process. The novel approach considers the blade to consist of a collection of parametric pre-defined blocks. This allows wind turbine blade models consisting of shell elements, solid elements or combinations to be created. By including the tools to accurately partition the outer mold layer, create the required offset surfaces and calculate accurate element-wise material orientations, a high level of detail and fidelity can be achieved.

Keywords: wind turbine blade, finite element modelling, solid mesh

1.1 Introduction

Wind turbine blade designs have been increasing in size during the last decades. They are complex structures, both in terms of shape and layup of composite materials. The rotor is at the very beginning of the energy conversion chain, turning airflow into mechanical energy. Consequently, the blades are at the beginning of a cost cascade system. For example, reducing the blade mass allows for cost savings in many other turbine components. Meanwhile, the aerodynamic performance directly contributes to the overall cost of energy (COE) of the turbine. As a result, there is great value in optimizing blades. Nevertheless, current wind turbine blades are often designed with relatively high safety factors. However, relatively large

numbers of repairs and early replacements are required ("Blade failure and load monitoring," 2008; Campbell, 2015). While many issues are related to the used manufacturing processes (Cairns et al., 2011; Nielow, 2014), this also indicates a need for detailed structural analysis to improve the understanding of the structure's behavior. This is possible by means of detailed finite element (FE) analysis. In industry this is often used to verify the stiffness, strength and stability of the design. The analyses allow a full strain field to be calculated, showing hotspots and allowing the calculation of fatigue behavior. Typical blade models use shell elements at the outer mold layer (OML). The OML surface is known from the aerodynamic shape of the blade and is typically available as a CAD file. Furthermore, the surface is independent of the layup. OML shell models are found to accurately predict strains and displacements of blades in bending as well as their flat and edge-wise Eigen frequencies. However, there are limitations. First off, these models do not contain an inside surface. As a consequence, the modelling of interior features lacks in accuracy. For example, the shear webs and adhesive bonds are attached to the outside surface. This does not align with reality. Similarly, the adhesive bonds cannot attach to the inside surface. In (Branner et al., 2007) an attempt was made to resolve this issue by scaling the stiffness of the adhesive to compensate for the geometrical inaccuracy. Alternatively, in (Haselbach, 2017) the adhesive at the trailing edge was modelled with solid elements that had correct dimensions and was attached to the laminate using a series of distributing couplings. Nevertheless, including the trailing edge adhesive is important to calculate the buckling reserve of the trailing edge panels (Bak et al., 2012). Furthermore, (Laird et al., 2005) discovered that shell elements with material offsets produced poor results when predicting torsion. This was found particularly for high material thickness-to-curvature ratio's. In (Griffith and Ashwill, 2011) an attempt was made to avoid this issue by scaling the thickness and stiffness of the laminate. The torsional behavior is particularly important for blade designs that undergo torsional deformation such as blades with a swept planform (Ashwill, 2010; Zuteck, 2002) or bend-twist coupling (Fedorov et al., 2012). Such behavior is used as a passive way to alleviate loads. Furthermore, for larger blades the torsional Eigen frequency becomes lower and may couple with other modes.

Alternative approaches have been suggested to model wind turbine blades. These include the use of shell elements at mid-thickness, solid elements or hybrid approaches where the skins of the sandwich structures are modelled with shell elements while the core material and adhesive bonds are modelled with solid elements. In (Hoyt, 2008) the torsional behavior of a swept wind turbine blade was investigated using a model consisting mainly of solid elements. Likewise, (Berring et al., 2007; Branner et al., 2007; Fedorov et al., 2012) used models obtained using different shell, solid and hybrid strategies to investigate the torsional behavior of a blade section with additional off-axis fibers and compared the results. The OML shell model produced poor torsional results while the solid and hybrid strategies were found to work best. In addition, various authors have also used continuum models in regions requiring more detail. In (Jensen et al., 2006) the behavior of a 34m blade under extreme loads was investigated. A shell model with elements on the OML was used, while a sub-model using both shell and solid elements was used. In (Wetzel, 2009) a solid model of a 44m blade was used to compare the damage tolerance of stressed spar and stressed shell blade designs. Damage introduced in the adhesive bonds would either result in a redistribution of stress or in "unzipping" of the adhesive bond resulting in blade collapse. It was found that stressed spar designs are more tolerant to damage in the adhesive. In (Chen et al., 2014) a model of the blade root and transition region consisting of a single layer of layered solid elements was used to investigate damage progression under ultimate load. In (Branner et al., 2016) a 34m wind turbine blade was modelled using second order layered solid elements. The blade was loaded in every direction up to the point of failure. In (Haselbach, 2017; Haselbach and Branner, 2015) a model consisting of shell elements for the laminate and solid elements for the adhesive at the trailing edge joint was used to predict the behavior of a blade under ultimate leading edge to trailing edge load.

Further, the materials used in modern wind turbine blades exhibit anisotropic properties. As a consequence, the orientation of the materials greatly affects the structural behavior (Chen et al., 2010). In industry, the level of accuracy of these orientations can be limited, since the orientations for the full blade are sometimes described by a single vector. In (Ashwill, 2010) material orientations are defined for every individual

element, based on two edges. The first orientation follows the leading edge, while the second is perpendicular to the blade radial direction. In (Bottasso et al., 2014) a single vector is defined per face, projection of each element normal onto the parametric blade surface allows calculation of the normal and an element-wise material orientation. Because of the level of detail required to obtain high fidelity blade models, various tools have been developed. An overview of existing tools is provided in Table 1. Frequently used tools are NuMAD (Berg and Resor, 2012) and FOCUS (ECN, 2016). Further, (Bonnet and Dutton, 2007) developed a tool to generate FE models using a python script. Also, a tool called BMT was developed by DTU to create solid models (Corona, 2013; Karakalas et al., 2016; Larsen et al., 2014). Further, (Bottasso et al., 2014) created a tool to obtain both shell and solid models in an automatic multi-tier optimization loop. Furthermore, (Hoyt, 2008) demonstrated a tool able to create solid models. However, the existing tools all have their limitations. First off, most tools are not easily extendible to account for additional details and many are limited to shell models. Some also do not include the capabilities required to accurately calculate key locations on the blade surface, but rather rely on the user to provide chord-ratios at a limited number of stations. Therefore, there is room for improvement in the tools for creating wind turbine blade models.

In this paper a novel approach to create FE blade models is presented, which allows both shell, solid and hybrid modelling strategies to be employed. The paper is structured in the following way: first, challenges for creating models other than shell OML models are described, next, an overview is given of how the challenge is broken up into smaller components and the employed solutions for different challenges are explained and demonstrated.

1.2 Challenges for creating models with solid elements

When models other than those consisting of shell elements positioned on the OML surface are created, new surfaces have to be calculated by offsetting from the OML. These surfaces are dependent on the layup. Since the total thickness at any point is the sum of the thicknesses of a discrete number of plies in the layup, the surfaces are in theory not continuous. This is especially true if the ply-drops are grouped to simplify the modelling process. In reality however, ply-stacks are given a gradual drop-off to avoid stress concentrations.

In (Laird et al., 2005) it is suggested to use a number of discontinuous surfaces and join them together with tie constraints. However, (Branner et al., 2007) discovered that this results in artificially stiff bending behavior. (Bottasso et al., 2014) on the other hand tried using continuous offset surfaces, removing the need for constraints.

One challenge when creating models consisting of continuum elements is that offsetting the blade OML surface can result in both global and local self-intersections (see Figure 1). Local self-intersections occur due to regions of high curvature in the original curve or surface, while global self-intersections result from different points on the curve or surface being offset to the same location. Offsetting is an active field of research and is important for CAD/CAM applications (Liu and Wang, 2011). The main challenges are typically to avoid intersections and maintain the parametrization of the base curve. In general, two main approaches exist. The first is to directly calculate the offset curve from the base curve and its normals and subsequently trim bad regions (Seong et al., 2006). While this maintains parametrization, the trimming process can be difficult. The other approach is to calculate a signed distance field and use that to evaluate a curve at the given offset. This approach avoids all intersections, but loses the original parametrization. As shown in Figure 1, local self-intersections are often present at the LE while global self-intersections tend to occur towards the TE. In (Ashwill, 2010) intersections at the TE core are noticed, but no solution is provided. It is worth noting that the global intersections are the result of an unrealistic layup in certain regions. This is also the case for models using shell elements, but often does not become apparent. Another challenge in creating solid models is the trailing edge region. Specifically, in the area where the transition is made from a circular root section to an airfoil shaped section. The difficulty here is that different faces are connected by the adhesive, as can be seen in Figure 1. Furthermore, a sudden transition is undesirable for the sake of mesh quality. Because of this difficulty, the transition region was not modelled in (Ashwill, 2010). In both BMT and (Bottasso et al., 2014) a TE configuration, which offsets the pressure and suction side panels according to the bisector is used. The same configuration can be used along the full span of the blade. However, neither seem to incorporate the over-lamination of the adhesive. A further challenge is the correct

positioning of the webs. The position of the webs is initially calculated on the OML surface. However, if the normal is used for offsetting the surface, this no longer matches the plane onto which the shear web is supposed to reside. For this reason, simply offsetting along the normal is not sufficient. Instead an offset vector along the shear webs' reference plane vertical direction should be used. This can be seen in Figure 2.

1.3 Materials and methods

The novel approach is implemented as an object-oriented software tool. This tool is able to generate full 3D FE models of wind turbine blades. It consists of a series of modules that take care of the individual model creation steps. While it is a standalone tool, it was developed in python for fast implementation. To simplify the challenge of creating the models, a divide and conquer approach is used. Instead of considering the blade as a single entity, it is considered in the novel approach as a collection of pre-defined parametric blocks. Each block consists of a number of components that each have their geometry and layup. To account for different regions and modelling strategies, a library of block types is available. Each block type has a different configuration and serves a single or two opposing panels (one on the PS and one on the SS). For example, there is both a block type that creates a single face from a panel (that is later meshed with shell elements) and a block type that creates a single cell (that is later meshed with solid elements). More advanced block types create multiple cells and faces through the thickness. In this way there are also block types creating a trailing edge by modelling the entities representing the laminate on the PS and SS as well as that on the TE side and the adhesive connecting them. The same goes for the shear webs and their flanges. A schematic overview of some different block types can be seen in Figure 3. Other software tools that are able to create models other than those with shell elements on the OML, typically consider a fixed pre-defined chord-wise topology for the blade. This facilitates the process of creating the mesh features. Other software tools that do not constrain the topology are typically only able to create OML shell models. In contrast, the approach allows very different layouts and is still able to create both OML shell, mid-thickness shell and solid models as well as combinations of those. Figure 4 shows an example of how a collection of blocks can be used to model a blade section.

1.4 Results

1.4.1 Software structure

The software is broken down in a number of modules able to handle the different tasks. In this paragraph, a brief overview is given. Further in the paper, specific features are discussed in detail. As a first task, a parametric surface is created from the OML shape. As a second task, this surface is partitioned. This is done in a two-step process. The surface is first partitioned by means of functions along the length of the blade and subsequently at a series of span-wise positions. The result is a “map” of the blade. This map represents the topology and consists of vertices, edges and panels. On this map, each ply in the composite layup can be assigned to the correct region. It is worth noting that this intermediate result is independent of the desired output model. Once the topology is clear, blocks can be assigned to the panels. This allows that the actual features such as faces and cells can be created. As final tasks, these features are meshed and material orientations can be calculated. An overview of the different stages in the modelling process can be seen in Figure 5.

1.4.2 High fidelity partitioning of the OML

A first challenge for producing high fidelity models is accurately partitioning of the OML surface. Existing tools often rely on the user to specify chord-ratios at a limited number of positions. A superior approach is to define functions on the OML surface, which can be evaluated at any span-wise position to accurately calculate partitioning positions. Furthermore, these functions need to represent positions in terms of arc-lengths because many plies are made of rolls of material with a constant width. The importance of this last statement can be demonstrated by a simple example. Assume that a blade has a main girder made from a roll of uni-directional fiber material with a constant width of 650mm. To model this blade, the boundary curves of the plies have to be calculated. In a fist approach, both boundary curves are defined by the intersection of the OML and a plane. The two planes are positioned 650 mm apart. In a second approach, one curve is calculated by the intersection of the OML with a plane, while the other is calculated by adding

an arc-length offset (of 650 mm) from the first curve. The resulting curves can be seen in Figure 6. While the curves seem similar, the difference reaches up to 41mm which is more than 6% of the width of the girder. Considering that this is the most important structural component, this deviation could have a significant effect. For this reason, in the presented approach, the OML surface is calculated so that it can be evaluated both in parametric uv-space (where u and v are in [0,1]) and parametric st-space, with s the span-wise position and t the circumferential position on the slice at position s. This allows curves to be calculated in arc-length space, resulting in accurate partitioning.

1.4.3 Topology of the blade as a map

As mentioned, partitioning of the blade results in a map, describing the topology. Unlike in other software, this does not fully define the final output since the assigning of blocks will determine what cells and faces are produced. At the map level, the layup can be assigned and blocks can be assigned to the desired regions. The map serves as a layer that considers the information that should be shared over multiple blocks. For example, the thickness of each component is calculated in every corner of every panel from the thickness values of the layups in the adjacent panels. This allows the blocks assigned to these panels to have matching thicknesses at their corners and create continuous meshes.

The layup is applied at the map level in an automated fashion. Regions are specified in terms of the bounding keylines and span-wise positions. This information makes it possible to determine rapidly which panels belong to the region. This approach differs from most other software tools, where typically the layup is specified at the level of the features. The advantage lies in the fact that in highly detailed models, the number of panels is typically much higher than the total number of layers in the layup. Furthermore, the number of panels may be modified to change the level of detail without requirement to alter the layup definition.

1.4.4 Creating a blade model from blocks

To obtain a useful model from a collection of pre-defined blocks, the adjacent blocks have to be compatible. This means that the interfaces between adjacent blocks should match, so that a continuous mesh can be formed. Compatibility is on one hand determined by the type of block, in the sense that there are different families of compatible blocks. An example of such a family are shell blocks, since they are compatible with other shell blocks, but not (directly) with solid blocks. In addition, the vertices on the edges that are adjacent to other blocks have to coincide with the vertices of those blocks so that they are stitched together and a single compatible mesh can be formed. This requires that both the offset normal and distance are identical for the adjacent blocks. Therefore, at the map level, the component thicknesses and offset normals are calculated in every corner, based on the values of the adjacent panels. These values are then used by the individual blocks. Examples of resulting meshes can be seen in Figure 7. Both first and second order meshing is available while both structured and transitional meshes can be created. Furthermore, both solid, shell and solid-shell elements can be created.

The presented approach is very flexible, since changing the way a specific part of a blade is modelled is as simple as assigning a different block type. Furthermore, the assignment of blocks is the final user input, meaning that this does not require any other inputs to be modified. In addition, the approach is easily extendable. All that is required to provide additional functionality is adding new block types. Furthermore, it is very straightforward to create detailed sub-models of specific regions of interest. Also, the block approach allows for flexibility in topology which is typically not available in other software tools able to create solid blade models. This approach is also very general and could therefore also be applied to the model creation process of different components such as for example airplane wings.

To create solid models, the inner surface has to be created by offsetting from the OML surface. However, unlike in most CAD/CAM applications, the offset distance is not uniform for the full shape. Different thicknesses are required for different segments and continuous variations in thickness are desired. However, maintaining parametrization is desired to some extent in order to reach a good quality mesh. This requires

that the shape of elements stays within certain bounds from regular bricks and wedges. In (Ashwill, 2010) the mesh is directly extruded inwards from the mesh on the OML surface. In (Bottasso et al., 2014) it is pointed out that this is not a good approach. Instead this is done at the geometry level. Offset surfaces are calculated and used to create faces or cells. However, as mentioned earlier, the offsetting process can be challenging. Therefore, the process is simplified with the approach shown in Figure 8. Instead of offsetting a full surface, the offset surface is calculated as a sequence of offset curves. Furthermore, the offset curves are calculated in the plane of the considered blade section, by projecting the offset normals onto the plane and compensating the offset thickness. Additionally, the offset curves are calculated as a sequence of offset segments. First, the bounding vertices of the offset curve are calculated by directly offsetting from the base curve. Next, a smooth connecting curve is calculated considering the distance field. In this way self-intersections are avoided in between the bounding vectors while the parametrization is largely maintained. This allows the creation of a good mesh and accurate offset curves. In addition, this solves another challenge which was mentioned earlier, namely the need to offset along a different vector than the normal vector. This is both the case for vectors at the TE and vectors of a shear web. With the given approach, the offset vectors are simply modified to have the desired orientation. The offset distance is then automatically compensated to result in the same material thickness and offset curves connecting the vectors are calculated considering the distance field.

1.4.5 Material orientations

The most accurate material orientation available with most FE solvers is by means of a local orientation system for every element individually. An approach was developed to calculate these orientations based on keyline definitions. The assumption is made that fibers that were parallel in the original fiber mat stay parallel in terms of arc-length when placed on the blade mold. Therefore, parallel fibers will be parallel to a ply edge. This means that shearing within the fiber mats is neglected. However, these effects are assumed to be very small. Using this assumption, an orientation system can be defined based on any keyline. The keyline can be evaluated at any position on the blade surface and arc-length parallel curves can be created for any

position on the OML. An example can be seen in Figure 9. Therefore, at any position on the OML, from this keyline the 1-direction of the material can be calculated as a 3d vector. Together with the normal which is evaluated from the OML surface, a full material orientation system is calculated. Using this approach, as many orientations can be created as there are keylines. Subsequently, every component of every block can be assigned a (different) orientation using this method.

1.4.6 Additional possibilities

The software also includes solid blocks that can have a cell representing the wet layup (over lamination of the adhesive bonds). This can be seen in the examples shown in Figure 4 and Figure 10. However, this cell can also be used for different purposes, such as to represent icing on the blades or the rubber layer usually placed in between a blade and fixtures used for load introduction during static testing. Further, more advanced web blocks are possible, containing a circular, elliptical or V-shaped cut-out. In addition, these web blocks could consist of a much larger number of components (faces or cells with a different layup) to include more design details as shown in Figure 10. Furthermore, the block approach provides a very straightforward tool for using global-local sub-modelling. This can be done by first creating a global shell model and subsequently considering a more refined (solid) model for the region of interest. Or, ideally, a coarse solid global model can be used and regions of interest can be investigated further with a refined local solid model. Furthermore, in the future additional blocks could be added that contain a layer of cohesive elements at the interface of the adhesive and the laminate. Additionally, the software includes tools to accurately calculate both the mass and material distribution in the blade. This serves as a tool to compare the model with the design and find any errors in the user input. The typical runtime of the software is highly dependent on the level of detail in the user inputs. For a model consisting of over 8000 panels in the map, resulting in a solid model of 184 105 second order solid elements, the runtime is about 24 minutes on a laptop with a 2.4Ghz quad-core processor and 8Gb of RAM. The calculation time is spent on the OML surface (1%), keylines (2%), creating the map (15%), calculating geometry for the blocks (7%) and meshing (75%).

1.4.7 Demonstration of possible applications

To show examples of possible applications and possibilities of the tool, global and local models are made and analyzed. This can be seen in Figure 11. First, a full blade is modelled using the software. A global solid model is produced and analyzed under a static load case. In addition, a refined local model is produced, representing a 1 m long section. This can be done by requesting a different output from the software. The nodal displacements of the global model are applied as boundary conditions to the local model using the sub-modelling technique. The resulting strain distribution can be seen in Figure 12. In this way, unlike with conventional shell models, a very detailed, general strain field is obtained, including in the thickness direction of the laminate. Furthermore, by modifying a single keyline, a locally reduced bond with can be introduced in the model, as presented in Figure 13. Using this approach, various manufacturing flaws could be investigated.

1.4.8 Comparison with existing tools

While a variety of tools exist to create wind turbine blade FE models, the newly presented tool differs in the following ways:

- The new approach allows models with a variety of different configurations to be generated, from the same input.
- The tool is stand-alone and does not rely on other pre-processor tools.
- Unlike with some existing tools, all components required to obtain highly detailed models are present. Specifically, the ability to calculate accurate partitions and material orientations.
- The tool's capabilities can easily be extended by defining new block types.

1.5 Conclusion

The increasing dimensions of wind turbine blades, cascade effects in the costs of the turbine and current failure ratio's make the use of advanced FE modelling of the blades desirable. Current modelling efforts appear to be limited in detail and fidelity because of the difficulty to obtain them. The newly presented

approach divides the modelling process in a number of steps and allows for a variety of models to be created.

The approach allows:

- Creation of the OML shape
- Accurate partitioning of the OML shape
- Creating models by combining pre-defined parametric blocks
- Assigning the layup and blocks at the map level, enabling:
    - Shell models (on the OML, at mid-thickness or on the inside surface)
    - Layered continuum (solid or solid-shell) models with adhesive bonds at the geometrically correct locations
- Simple global-local modelling approaches
- Calculating element-wise material orientations based on keylines

The approach is flexible since it allows different topologies to be modelled. Likewise, different outputs can be created by modifying only the user inputs in the last stage of the model creation process. In addition, the approach is highly extendible. Additional functionality can be created by simply adding a new type of block to the available collection. Furthermore, the tool gives possibilities to investigate the effect of manufacturing flaws. One approach to do this is using the sub-modelling method, for which the presented tool is well suited.

Acknowledgments: The work leading to this publication has been supported by VLAIO (Flemish government agency for Innovation and Entrepeneurship) under the SBO project "OptiWind: Serviceability optimisation of the next generation offshore wind turbines" (project no. 120029).

Table 1: Overview of existing tools for the creation of 3D FE models of wind turbine blades.

Tool	Pre-processor	Key locations	Laminate modelling				Adhesive		
			Shell (BOT)	Shell (MID)	Shell (TOP)	Solid	Web joint	TE joint	LE joint
FOCUS (ECN, 2016)	Stand-alone	Detailed	Yes	-	-	-	-	-	-
NuMAD (Berg and Resor, 2012)	ANSYS ("ANSYS," n.d.)	Chord-fraction based	yes			-	-	-	-
BMT	PATRAN ("Patran," n.d.)	?	-	-	-	yes	yes	yes	-
Dutton (Bonnet and Dutton, 2007)	Stand-alone	?	yes	-	-	-	-	-	-
Botasso (Bottasso et al., 2014)	Hypermesh (Altair Engineering, 2017)	?	yes	yes	yes	yes	yes	yes	-
NSE Blademesher (Ashwill, 2010; Hoyt, 2008)	Stand-alone	Chord-fraction based	-	-	-	yes	yes	yes	-

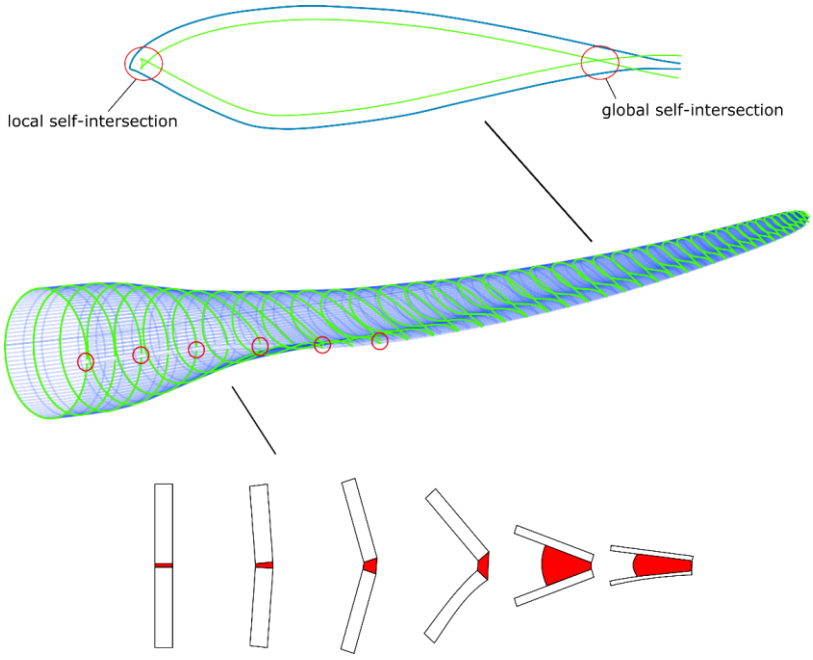

Figure 1: (top) Airfoil section and offset curve containing local (at the LE) and global (at the TE) self-intersections (middle) typical shape of a wind turbine blade (bottom) detail of the trailing edge shape at different positions along the transition from the root to an airfoil shape.

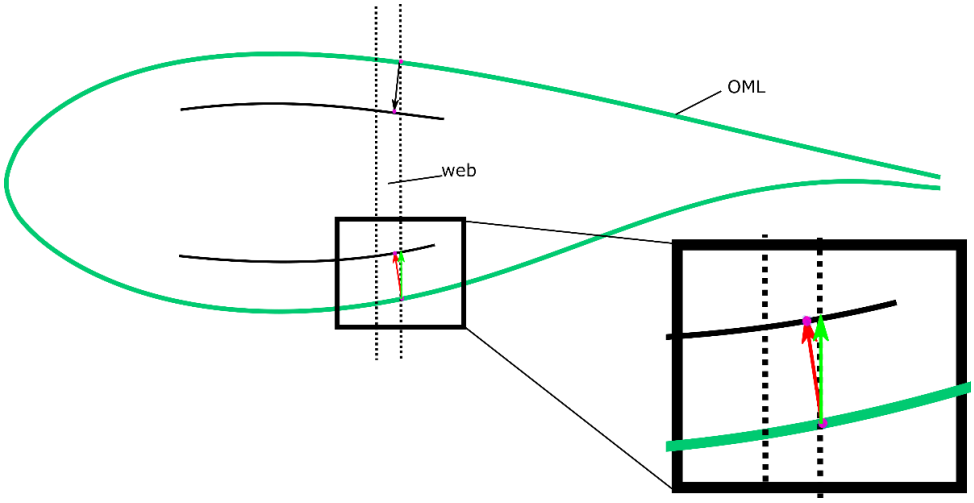

Figure 2: Schematic view of the location for a shear web. The intersection of the reference plane with the outer mold layer (OML) is first calculated. An offset along the normal (red) of the OML does not result in the intended shear web. Instead an offset along the vertical direction of the shear web (red) is required.

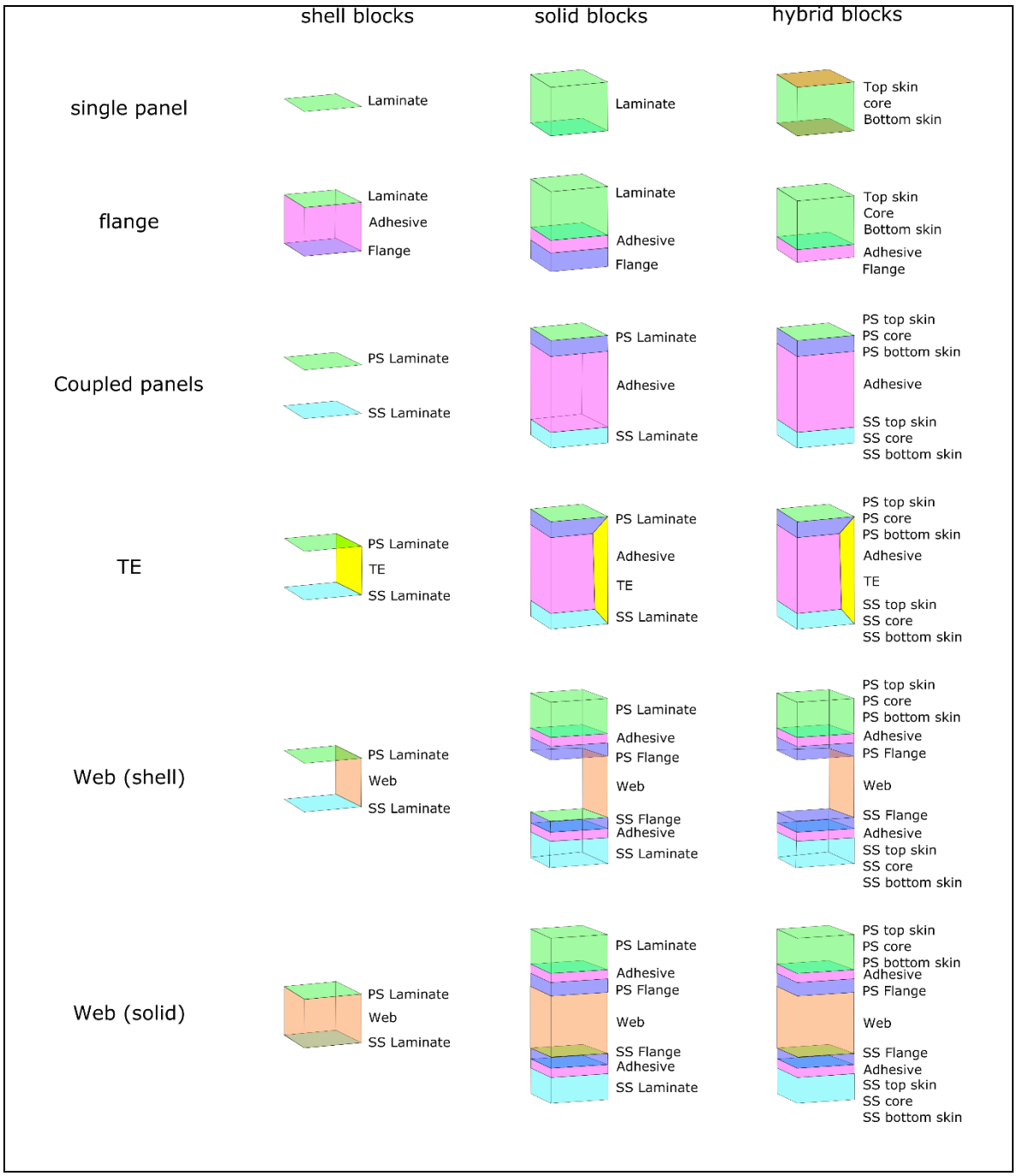

Figure 3: Schematic overview of blade blocks. Three main compatible categories are shown (shell, solid, hybrid). A single panel block is assigned only to a single panel, while other blocks are assigned to a combination of a panel on the SS and a panel on the PS. Various blocks are available to model different features.

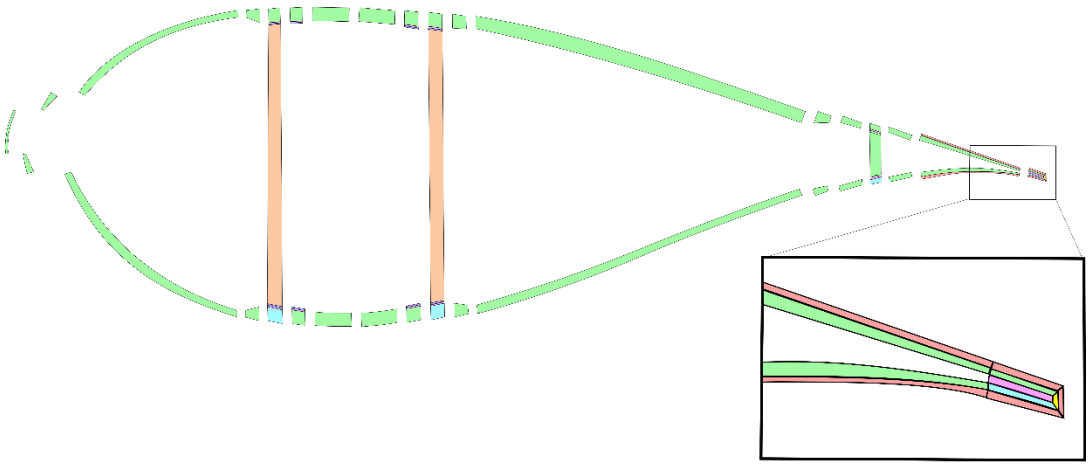

Figure 4: Example of how a number of compatible blocks result in a cross-section of a high fidelity solid model..

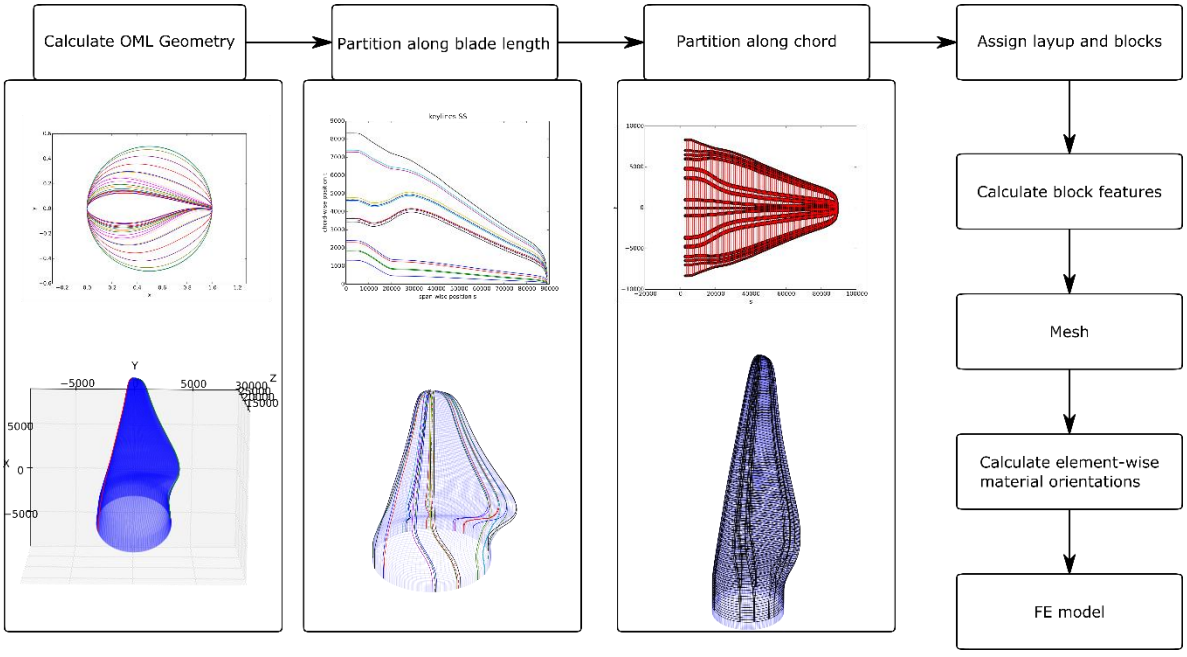

Figure 5: An overview of the different stages of the process of generating a FE model of a wind turbine blade with the proposed approach.

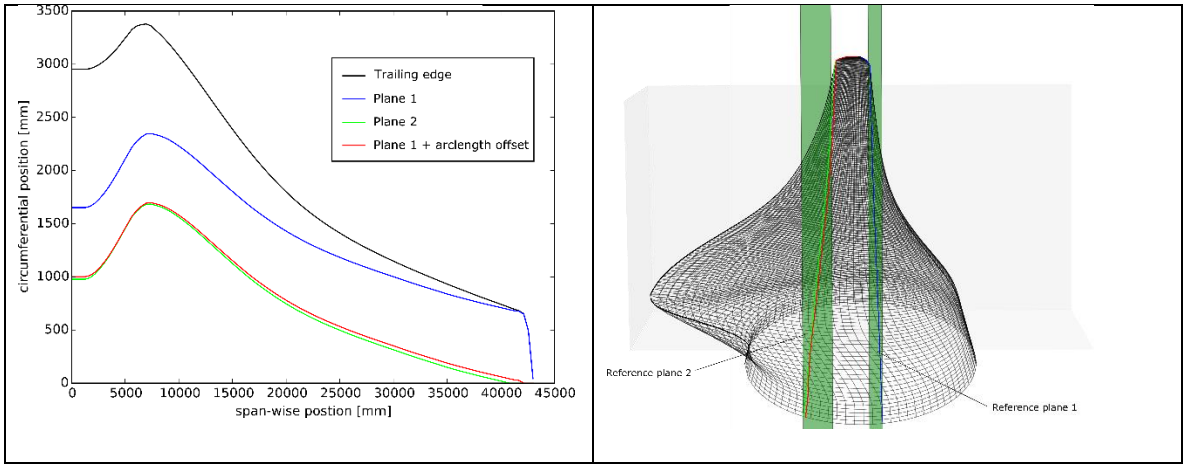

Figure 6: Comparison of methods to calculate the boundary curves of a girder with a constant width of 650 mm. The boundary on the LE side is calculated from the intersection with a plane. The boundary on the TE side is calculated in one approach by means of a second reference plane and in another approach by offsetting from the curve on the LE side. The difference in width reaches up to 41 mm.

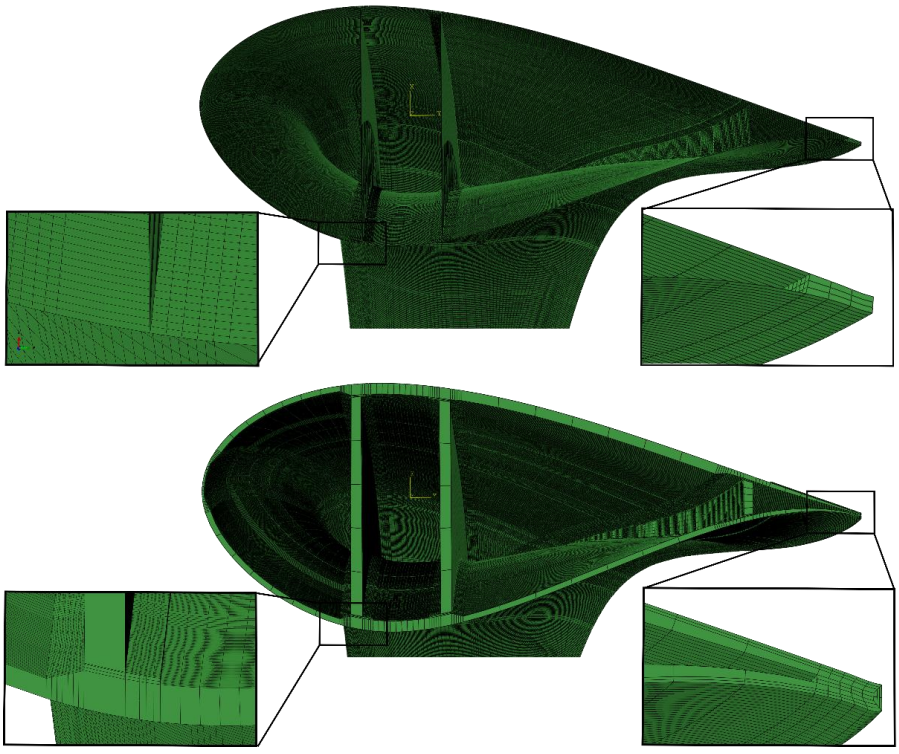

Figure 7: Meshes produced by the software along with details of the trailing edge joint and web-girder connections. (top) Shell output with solid elements to model the adhesive. (bottom) Second order solid output.

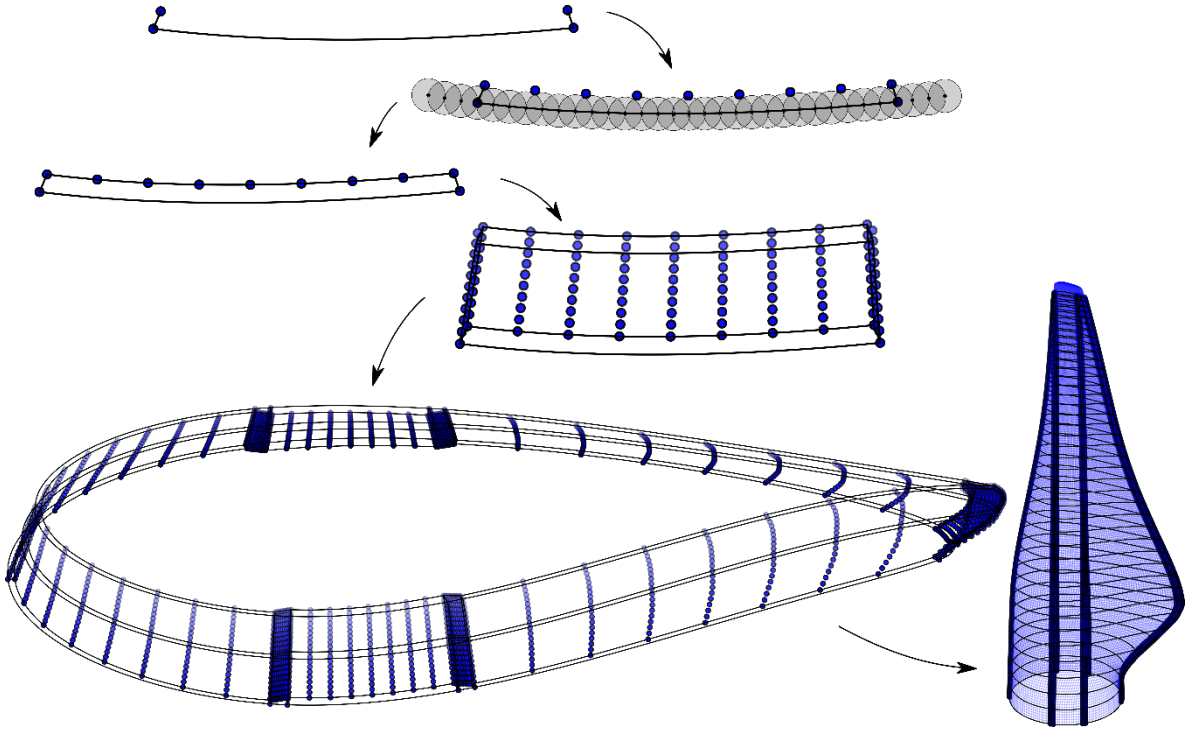

Figure 8: The offsetting of slice segments is used to create offset surfaces. These surfaces are used to create solid blocks.

The blocks are subsequently combined to create a full model.

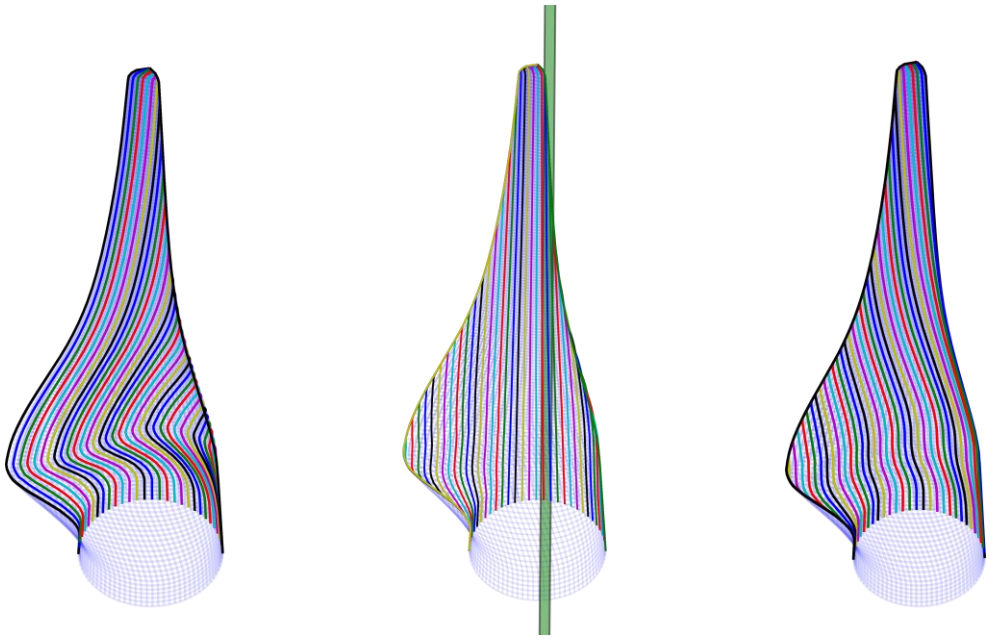

Figure 9: Curves representing parallel fibers according to the arc-length un-wrapping of the OML surface. (left) Curves parallel to the TE. (middle) Curves parallel to the intersection of the OML with a plane. (right) Curves parallel to the LE.

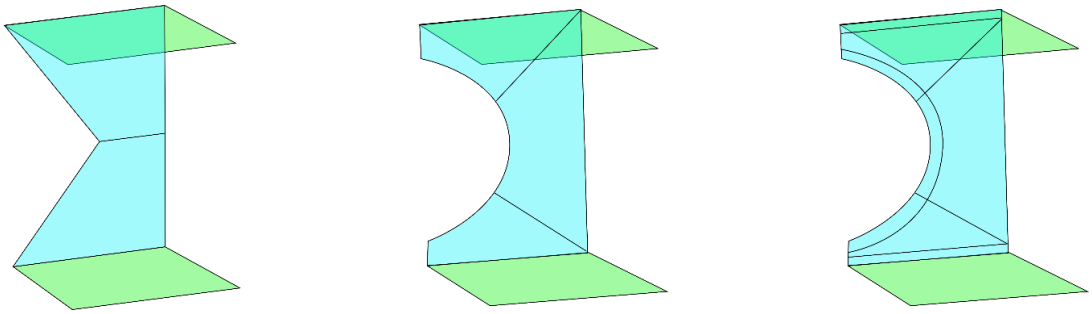

Figure 10: Schematic examples of other web block configurations. (left) V-cut out (middle) Elliptical cut-out (right) Elliptical cutout with more components to provide additional detail.

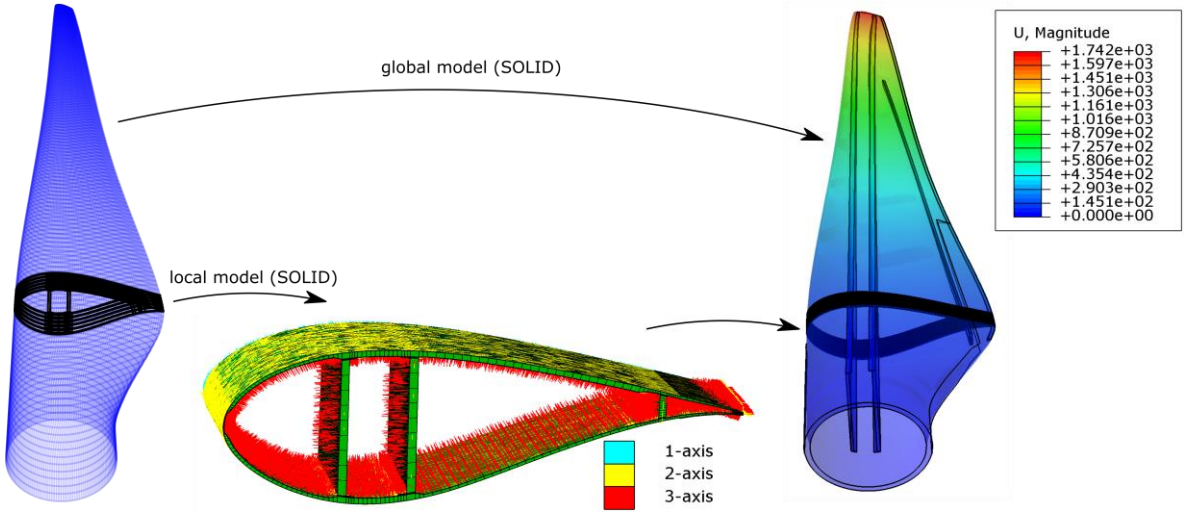

Figure 11: An example of a global-local approach which is feasible using the novel tool. The full blade is modelled using the software. A global solid model is created for the full blade and a local solid model is created for a 1 m long section. The global model is used in a static analysis and the nodal displacements are used as boundary conditions in the sub-model.

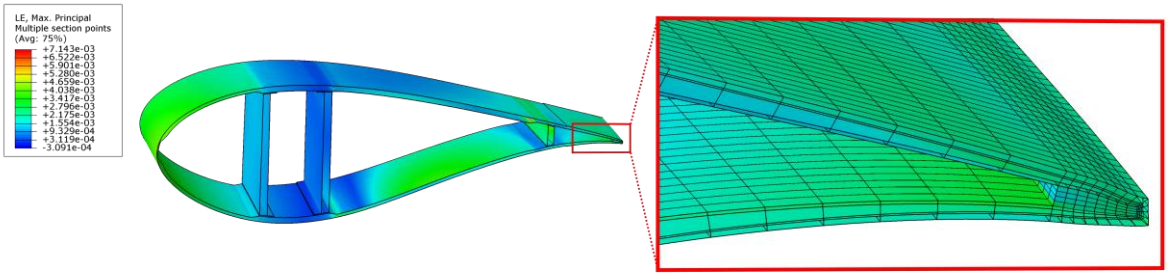

Figure 12: Contour plots of the maximum principal strain values on the local blade model. Stress values are available in all directions including the thickness direction. A close-up view of the trailing edge joint is provided with the mesh visible.

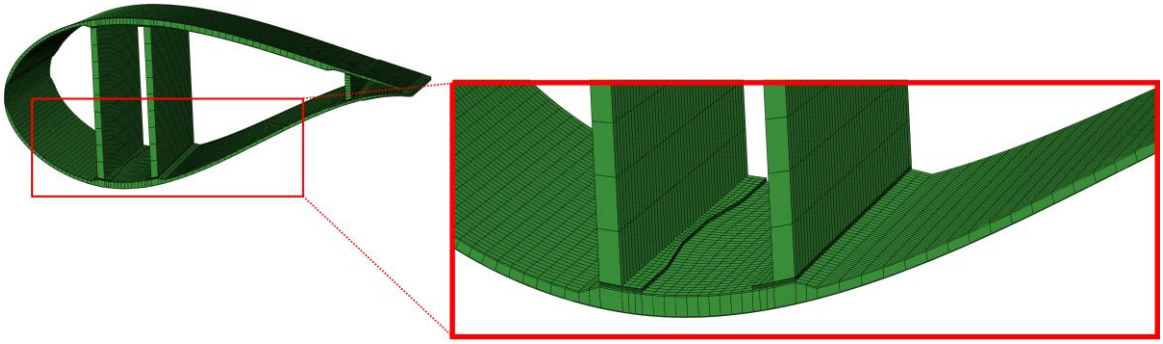

Figure 13: Plot of the mesh of a modified sub-model that has a local reduction in bond width at the joint of the LE shear web.

1.6 Bibliography

Altair Engineering, 2017. HyperMesh [WWW Document]. URL http://www.altairhyperworks.com/product/HyperMesh (accessed 4.4.17).

ANSYS [WWW Document], n.d. URL //www.ansys.com/ (accessed 2.6.18).

Ashwill, T., 2010. Sweep-Twist Adaptive Rotor Blade: Final Project Report (No. SAND2009-8037). Sandia National Laboratories.

Bak, C., Bitsche, R.D., Yde, A., Kim, T., Hansen, M.H., Zahle, F., Gaunaa, M., Blasques, J.P., Dossing, M., Wedel Heinen, J.-J., Behrens, T., 2012. Light rotor: the 10 MW reference wind turbine, in: Proceedings of EWEA 2012 - European Wind Energy Conference & Exhibition. European Wind Energy Association (EWEA),.

Berg, J., Resor, B., 2012. Numerical manufacturing and design tool (NuMAD V2. 0) for wind turbine blades: User's guide. Sandia Natl. Lab. Albuq. NM Tech. Rep. No SAND2012-728.

Berring, P., Branner, K., Berggreen, C., Knudsen, H.W., 2007. Torsional performance of wind turbine blades-Part 1: Experimental investigation, in: 16th International Conference on Composite Materials.

Blade failure and load monitoring [WWW Document], 2008. URL https://www.windpowermonthly.com/article/953663/blade-failure-load-monitoring (accessed 12.28.17).

Bonnet, P.A., Dutton, G., 2007. Parametric Modelling Of Large Wind Turbine Blades, in: Abaqus UK Regional User Meeting.
Bottasso, C.L., Campagnolo, F., Croce, A., Dilli, S., Gualdoni, F., Nielsen, M.B., 2014. Structural optimization of wind turbine rotor blades by multilevel sectional/multibody/3D-FEM analysis. Multibody Syst. Dyn. 32, 87–116.
Branner, K., Berring, P., Berggreen, C., Knudsen, H.W., 2007. Torsional performance of wind turbine blades–Part II: Numerical validation, in: 16th International Conference on Composite Materials. pp. 8–13.
Branner, K., Berring, P., Haselbach, P.U., 2016. Subcomponent testing of trailing edge panels in wind turbine blades, in: Proceedings of 17th European Conference on Composite Materials.
Cairns, D.S., Riddle, T., Nelson, J., 2011. Wind turbine composite blade manufacturing: the need for understanding defect origins, prevalence, implications and reliability (No. SAND2011-1094).
Campbell, S., 2015. Annual blade failures estimated at around 3,800 [WWW Document]. Wind Power Mon. URL https://www.windpowermonthly.com/article/1347145 (accessed 12.28.17).
Chen, J., Hallett, S., Wisnom, M.R., 2010. Modelling complex geometry using solid finite element meshes with correct composite material orientations. Comput. Struct. 88, 602–609. https://doi.org/10.1016/j.compstruc.2010.02.004
Chen, X., Zhao, W., Zhao, X., Xu, J., 2014. Failure Test and Finite Element Simulation of a Large Wind Turbine Composite Blade under Static Loading. Energies 7, 2274–2297. https://doi.org/10.3390/en7042274
Corona, A., 2013. Quantitative sustainability assessment of bio-based materials for wind turbine rotor blades (MSc in Materials Engineering). Technical University of Denmark.
ECN, 2016. FOCUS6 - The integrated wind turbine design suite.
Fedorov, V., Berggreen, C., Krenk, S., Branner, K., 2012. Bend-Twist Coupling Effects in Wind Turbine Blades. DTU Wind Energy, Denmark.
Griffith, D.T., Ashwill, T.D., 2011. The Sandia 100-meter all-glass baseline wind turbine blade: SNL100-00 (No. SAND2011-3779).
Haselbach, P.U., 2017. An advanced structural trailing edge modelling method for wind turbine blades. Compos. Struct. 180, 521–530. https://doi.org/10.1016/j.compstruct.2017.08.029
Haselbach, P.U., Branner, K., 2015. Effect of trailing edge damage on full-scale wind turbine blade failure, in: 20th International Conference on Composite Materials.
Hoyt, D.M., 2008. Rapid FEA of Wind Turbine Blades - Summary of NSE Composites' structural analysis capabilities for blades.
Jensen, F.M., Falzon, B.G., Ankersen, J., Stang, H., 2006. Structural testing and numerical simulation of a 34m composite wind turbine blade. Compos. Struct. 76, 52–61. https://doi.org/10.1016/j.compstruct.2006.06.008
Karakalas, A., Machairas, T., Solomou, A., Saravanos, D., Lachenal, X., Weaver, P.M., Berring, P., Branner, K., 2016. New morphing blade section designs and structural solutions for smart blades (No. D2.23), INNWIND.EU.
Laird, D., Montoya, F., Malcolm, D., 2005. Finite Element Modeling of Wind Turbine Blades. American Institute of Aeronautics and Astronautics. https://doi.org/10.2514/6.2005-195
Larsen, G.C., Berring, P., Tcherniak, D., Nielsen, P.H., Branner, K., 2014. Effect of a damage to modal parameters of a wind turbine blade, in: EWSHM-7th European Workshop on Structural Health Monitoring.
Liu, S., Wang, C.C.L., 2011. Fast Intersection-Free Offset Surface Generation From Freeform Models With Triangular Meshes. IEEE Trans. Autom. Sci. Eng. 8, 347–360. https://doi.org/10.1109/TASE.2010.2066563
Nielow, D., 2014. Prüfstand für die Evaluation der Betriebsfestigkeit von Rotorblattschalensegmenten. Presented at the Rotorblätter von Windenergieanlagen Wind turbine rotor blades 6th Technical Conference, Essen.
Patran [WWW Document], n.d. URL http://www.mscsoftware.com/product/patran (accessed 2.6.18).

Seong, J.-K., Elber, G., Kim, M.-S., 2006. Trimming local and global self-intersections in offset curves/surfaces using distance maps. Comput.-Aided Des. 38, 183–193. https://doi.org/10.1016/j.cad.2005.08.002

Wetzel, K., 2009. Defect-Tolerant Structural Design of Wind Turbine Blades. Presented at the 50th AIAA/ASME/ASCE/AHS/ASC Structures, Structural Dynamics, and Materials Conference, Palm Springs, California. http://dx.doi.org/10.2514/6.2009-2409

Zuteck, M., 2002. Adaptive blade concept assessment: curved planform induced twist investigation (No. SAND2002-2996). Sandia National Laboratories.